

# Simulation of Non –Evaporating Diesel Sprays and Comparison with Empirical Correlation

Ishtiaq A. Chaudhry<sup>1\*</sup>, M.R. Mirza<sup>1</sup>, M.J. Rashid<sup>1</sup>

<sup>1</sup>Department of Mechanical Engineering, University of Engineering and Technology, Lahore Pakistan

\* Corresponding Author: Ishtiaq Ahmed Chaudhry ishtiaqach@uet.edu.pk

## Abstract

*Non-evaporating diesel sprays are simulated using sub models given in Fluent software. Meshing of the CFD model is done using Gambit software before transmitting it to Fluent software. The modeling is carried out using cold bomb conditions under variable gas pressure, density, nozzle diameter and fuel injection pressure, but maintaining gas temperature as atmospheric. The simulated penetration rate and spray tip velocity are compared with existing experimental data. An excellent match is found between simulation results and published correlation. The CFD simulation is found to be highly dependent on injection parameters and operating conditions.*

**Key Words:** Non-evaporating diesel sprays, penetration rates, CFD modeling of sprays, Fluent, Simulation, Penetration rate

## Nomenclature

$P_{inj}$	Injection Pressure
$P_{ch}$	Chamber Pressure
$X_p$	Penetration Distance
$\Delta p$	difference between injection pressure and chamber pressure
$d$	nozzle diameter
$\rho_a$	chamber air density at any given pressure but maintaining the atmospheric temperature
$\rho_g$	gas density in the chamber at said pressure and temperature
$t$	time span measured from the onset of fuel injection

## 1. Introduction

The very first requirement to effectively use a computational fluid dynamics model is to prepare a 3D physical geometric model of the problem. Analysis of the fuel spray process involves specification of chamber space like bore and stroke of an internal combustion engine. Fluent software needs geometric meshing which in the present case is carried out using commercially available Gambit software. Construction and break down of the physical models, meshing and file generation can be done using Gambit. As Gambit is written for Linux environment, its use requires additional software known as Exceed.

## 2. Modeling

### 2.1 Mesh Construction

For the construction of geometrical mesh, bore and stroke are chosen as 77 mm and 85 mm. The construction of structured mesh requires following of the systematic approach like bottom to top meshing technique. Figure 1 show the systematically constructed mesh used in the

present simulation. The mesh refinement is done to achieve optimized condition by controlling the total number of cells using sizing function. The generated mesh file is made compatible for making it importable by the Fluent software. Mesh usefulness is decided by simulation (Fluent) using dummy data. Starting cell size of mesh  $0.2 \times 10^{-3} m$  and limiting cell size of  $8 \times 10^{-3} m$  with a growth rate of 1.05 are found useful for the purpose of simulation; Distance is taken as the extents of cylinder.

### 2.2 Injection Modeling

The simulation of spray requires specification of the Injector model. The compression ignition engines use multi-hole injector. The group type single-hole injector is chosen for the simulation purposes, which uses information including nozzle diameter, mass flow rate, initial droplet size, droplet size distribution, droplet velocity and position of injector. All such information completely defines the fuel injection model.

A Fiat single-hole 0.25mm diameter orifice nozzle, used by Mirza [1], is chosen as a reference case and use is made of his published experimental results on fuel injection characteristics of the pump-line-injector combination using distribution type commercial fuel pump. The simulation results on spray penetration rates are compared with the empirical correlations.

Rosin-Rammlar distribution is used for particle size distribution with initial and final particle size of  $1 \times 10^{-6} m$  and  $5 \times 10^{-5} m$ , respectively with mean diameter  $26.8 \times 10^{-6} m$  and a spread parameter of 2 according as has been suggested by Saario [2]. Co-efficient of discharge is taken as 0.39 as reported by Hiroyasu and Arai [5], Mirza and Baluch [7] for the calculation of fuel mass flow rate through the injector.

### 2.2.1 Droplet Collision Model

Injection of fuel is assumed to consist of N number of particles. The droplet collision model handles the effective computation of the possibility that any two particles out of N particles will collide by introducing the concept of parcel. This reduces the computational cost several thousand times. Parcel is defined as a group of particles, which behave in a similar fashion collectively. Fluent uses O'Rourke's algorithm [3] to estimate probability of collision and its outcome in the form of coalescence or bouncing.

The model assumes that collision frequency is very small as compared to the time step. To adjust this, particle length scale is to be adjusted according to the distance traveled by the particle in present time step. Because of the assumption of collision in the same cell, grid dependant artifacts like stratification of particles can be seen. To avoid such situation a more refined grid should be adopted.

### 2.2.2 Spray Breakup Model

Fluent software provides the option to use two different models for the breakup of fuel spray called TAB (Taylor Analogy Breakup) model and Wave model. TAB model is reported to be widely applicable model for many engineering situations. The analogy is created between an oscillating and distorting droplet and a spring mass system. The break up model assumes the division of a large particle into small particles. Wave model is an alternative to the TAB model for high-Weber-number flows, based on the work of Reitz [4]. Wave model considers the breakup of the droplets to be induced by the relative velocity between the gas and liquid phase. The model also predicts the parameters like particle diameter and particle velocity after break up. The Wave model is used in the present work [fluent]. Advanced version of TAB model, called E-TAB is not available in Fluent software.

### 2.2.3 Drag Model

The Dynamic drag model calculates and updates the droplet drag coefficient, accounting for variations in the droplet shape in high Weber number sprays. The drag acting on a particle depends on the shape of particle. The model interpolates the drag of a particle by calculating the distorted shape between the shapes of a sphere and that of a flat disk, by making use of the drag co-efficient distribution, which is assumed linear [6].

## 3. Experimental Data

### 3.1 Correlations

There are a number of published single-line empirical and semi-empirical correlations  $t^{1/2}$  type for the penetration rates of diesel sprays based on the theory of gas jets. All such correlations have the disadvantage of over prediction of the initial nozzle tip zone. The 2-line correlation equation of Hiroyasu and Arai [5] assumes straight-line relationship

near the nozzle tip zone, also called the liquid phase zone; and the  $t^{1/2}$  type relationship for the spray tip or the vaporous zone. The research work of Mirza [1] narrates smooth blend of the initial liquid phase and the end vaporous zones, and is reproduced as under.

The basic  $t^{1/2}$  type correlation describes penetration rates of diesel sprays as follows, with over prediction of the initial liquid phase:

$$Xp = 3.8 \left( \frac{\Delta p}{\rho_a} \right)^{0.25} d^{0.5} t^{0.5} \quad (1)$$

Modification to the above equation, proposed by Mirza [1] is described as follows:

$$Xp = 3.8 \left( \frac{\Delta p}{\rho_a} \right)^{0.25} d^{0.5} t^{0.5} \tanh 4.1 \times 10^3 t \quad (2)$$

The added hyperbolic function smoothly blends the liquid and the vaporous zones of the spray jet. This correlation equation is taken as reference for the comparison of present simulation results. Mirza [1] has also reported the straight line fit to the initial near nozzle tip zone, in agreement to Hiroyasu and Arai [5] and Heywood [6]

$$\text{Fuel injection velocity} = 0.39 \left( \frac{2\Delta p}{\rho_f} \right)^{0.5} \quad (3)$$

### 3.2 Jet Breakup Mechanism

Jet breakup mechanism being the point of interest Mirza and Baluch [7] carried out an effort to investigate into it for both non-evaporating and evaporating sprays to realistically describe structure of sprays under variable chamber air / gas density due to variation in chamber pressure as well as chamber air / gas temperature, like Hiroyasu and Arai [5].

Mirza and Baluch [7], for non-evaporating sprays have defined the break up point as "point of intersection" of the following correlations which are for initial near nozzle tip zone and final spray tip zone, respectively.

$$X_{po} = C_1 \left( \frac{2\Delta p}{\rho_f} \right)^{0.5} t \quad (4)$$

$$X_{po} = C_2 \left( \frac{\rho_g}{\rho_a} \right)^{0.25} \left( \frac{\Delta P}{\rho_a} \right)^{0.25} d^{0.5} t^{0.5} \quad (5)$$

That is, for  $t = t_b$ ,  $X_{po} = X_b$ , equations (4) and (5) will give

$$t_b = \left[ \left( \frac{C_1}{C_2 \sqrt{2}} \right)^2 \tanh^2 4.1 \times 10^3 t_b^{0.5} \right] \left[ \frac{d \rho_f}{\Delta p \rho_a^{0.5}} \right] \quad (6)$$

Experimentally determined values of the constants  $C_1$  and  $C_2$  are 0.39 and 3.8, respectively, and  $\rho_a$  is the chamber air density at a given pressure but maintained at atmospheric temperature.

To solve it iteratively we can re-write equation (6) in the following form

$$t_b - \left[ \left( \frac{C_1}{C_2 \sqrt{2}} \right)^2 \tanh^2 4.1 \times 10^3 t_b^{0.5} \right] \left[ \frac{d \rho_f}{\Delta p \rho_a^{0.5}} \right] = 0 \quad (7)$$

Equation (7) is of the form  $f(t_b) = 0$ , the iterative solution of which gives the plot of  $f(t_b)$  against  $t_b$ , (Fig 4). The curve intersects horizontal  $t_b$  axis at 0.26 ms. The hyperbolic expression (equation 7) when simplified gives a value of 0.6, reducing equation (7), for their reference case, to the following form

$$t_b = \left[ 0.6 \left( \frac{C_1}{C_2 \sqrt{2}} \right)^2 \right] \left[ \frac{d \rho_f}{\Delta p \rho_a^{0.5}} \right] \quad (8)$$

Choosing  $C_1$  and  $C_2$  as 0.39 and 0.38 simplifies the equation (8) to

$$t_b = 28.7 \left[ \frac{d \rho_f}{\Delta p \rho_a^{0.5}} \right] \quad (9)$$

Constant of equation 3.2.6 is the same as reported by Hiroyasu and Arai [5] but in the denominator; density  $\rho_a$  differs from the density  $\rho_g$  [5]. Figure 2 shows comparison of the predictions of correlation equation (5) and the experimental results of Mirza [1]. It may be recalled that hyperbolic modification proposed by Mirza and Baluch [7] eliminates the over prediction of the initial nozzle tip zone of the spray.

In Figure 2, line through the experimental data points is the prediction of the modified correlation equation (5). Figure 2 show that the initial liquid phase of the spray can also be modeled by a straight-line relationship, which has been described above. Figure 3 shows the experimental data, the predictions of the original  $t^{1/2}$  type correlation equation (5) and the modified correlation equation (5) predictions super-imposed by the straight-line fit. The iterative solution of equation (7) gives the plot of  $f(t_b)$  against  $t_b$ , (Fig 4).

#### 4. Results and Discussions

For the purpose of simulation, the experimental test case of Mirza [1] is taken as reference. It uses mean injection pressure of 22 MPa to produce Diesel spray jet through a single hole 0.25 mm diameter orifice nozzle in the quiescent chamber maintained at 2.25 MPa and 290 K. Using a 3D co-ordinate system, Injection and cylinder axis are taken along y-axis. The 3D geometry of the chamber is defined such that the y-x plane at  $z=0$  will pass through the

injection axis. Fuel and air properties are tabulated in Table 1. Initial and boundary conditions are hence specified using the experimental case of Mirza [1]. Optimization of fuel injection velocity and particle diameter distribution is carried out, with upper limit using the following relationship reported by Mirza [1] and Hiroyasu and Arai [5] as described above.

The lower limit of injection velocity is obtained by optimization through simulation of the spray jet taking the experimental data reported by Mirza [1] described above, being 25 m/s in the present case. As has been described above, Rosin-Rammlar distribution is used for particle size distribution with initial and final particle size of  $1 \times 10^{-6}$  m and  $5 \times 10^{-5}$  m, respectively with mean diameter  $26.8 \times 10^{-6}$  m and a spread parameter of 2. Spread parameter defines the shape of size distribution curve, which is assumed exponential in the present case [Fluent v6.5].

For the purpose of simulation, the injector is placed normal to the horizontal with its injection axis in line with the cylinder axis. Unsteady formulation of simulation is carried out using segregated solver of Fluent. Validation of the model is made by cross checking the values of density, temperature and absolute pressure obtained by results with given operating environment.

Figure 9 shows the time histories of the evaporating and non-evaporating sprays. Close examination of Figure 9 shows a decrease of the order 20% in penetration rates with an increase in chamber air / gas temperature change from 290K to 800K. The reason to this effect may be explained by the evaporation of the fine vaporous spray tip zone by the hot environment. The reduction in simulated spray penetration under hot bomb conditions is in agreement with the findings of Dent [8], Hiroyasu and Arai [5] and also the predictions by the correlation of Mirza and Baluch [7].

Figure 10 and Figure 11 show histories of the spray penetration and spray tip velocity of the sprays under reference conditions of 22 MPa injection pressure, 2.25 MPa chamber air pressure and temperature of 290 K. Close elaborations of Figure 10 shows that the difference between empirical correlation and simulation results is 2-3% in the initial liquid phase zone. This difference reduces to 1% in the end vaporous zone of the spray jet. Further examination of Figure 11 shows that the simulated spray jet is highly instable in the first 0.6 ms period. The reason to this effect may be explained by the transient nature of the spray. Similar findings have been reported by Dent [8]. The experimental results of Mirza [1] also narrate akin findings but for the initial period of less than 0.4 ms.

Figure 5 shows the simulated results of the test case. The simulation results include the full range of particle

comprising the spray jet, the range being calculated by the software itself. The software, on the basis of distance from nozzle tip, automatically chooses the color of spray body. Figures 6 to 8 show the simulated spray shapes plotted at a randomly chosen time step of 0.5 ms measured from the commencement of fuel injection, to demonstrate the effect variation in fuel injection pressure, nozzle hole diameter and chamber air pressure, on spray shape. Close examination of these figures shows a reduction in spray tip penetration by an increase in the chamber pressure; increase in spray tip penetration by an increase in the injection pressure; and an increase in spray tip penetration by an increase in the nozzle diameter. All such trends are as expected. Note that we are only interested in the spray penetration rate along the axial direction of the cylinder while the radial spread of this particular spray is far less primary and so is the case with the provided correlation data. Secondly as far as figures 5 to 8 are apprehensive only the axial trend is of primary concern and the vital parameters along with the penetration rate are discussed in detail in the proceeding figures.

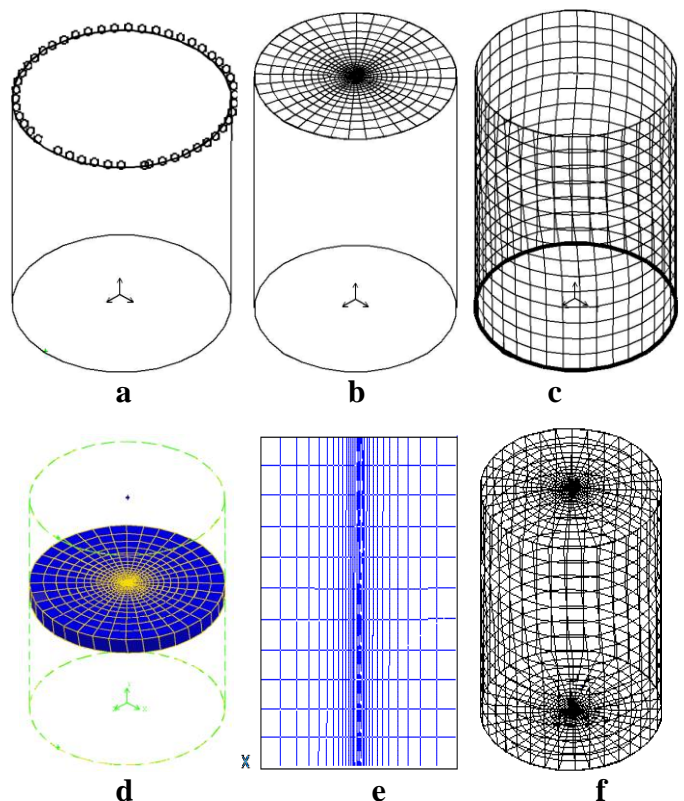
Figure 12 and Figure 13 show the histories of the spray penetration and their comparison for the non-evaporating case for different values of chamber pressure. Figure 12 illustrates that an increase in chamber pressure results in reduction of spray tip penetration. Figure 13 reveals that the most of the data points lie on the 45° line through the origin; showing an excellent match between the published correlation of Mirza and Baluch [7] and the simulated results. The over prediction trend by the correlation predictions is because of its natural tendency being of  $t^{1/2}$  type.

Figure 14 and Figure 15 show the spray penetration histories and their comparison for the non-evaporating case for different values of injection pressure. Figure 14 demonstrates an increase in penetration rates with an increase in injection pressure. The reason to this effect is explained by an increase in injection pressure and hence penetration velocity with an increase in injection pressure. Figure 15 shows the extent of match between correlation predictions and simulation results. The over prediction trend by the correlation predictions is because of its natural tendency being of  $t^{1/2}$  type. Figure 16 and Figure 17 show the variation in penetration rates with the variation in the injector nozzle diameter. Penetration rate increases with an increase in injector nozzle diameter the reason to which effect is explained by an increase in the initial spray jet momentum. There exists again an excellent match between the simulated and correlation predictions in the vaporous zone. The reason of slight disagreement of the initial liquid phase is the same as described above. Note that (b) part of each figure from 12 to 17 shows the mutual digression of

simulation and correlation lines and obviously closer the points to the line at 45° lesser the difference.

## 5. Summary and Conclusion

An excellent match is found between the simulated model and experimental data of Mirza [1]. There is a successive drop in spray tip velocity right from start of injection till end of injection. The assumption of constant velocity in the near nozzle zone is an approximation. The magnitude of the assumed constant velocity in the near nozzle tip zone requires compensation of the order 10 to 15% for the simulation by wave model, otherwise the model under-predicts penetration rates near the nozzle tip zone. However, the end vaporous zone is independent of the velocity compensation. The spray shape is found highly dependant on chamber density and particle size distribution. Axial penetration of spray decreases with increasing chamber density, and increases with increasing nozzle diameter. Number of particles required to maintain the spray shape increases as time step is increased. The wave mode offers excellent prediction of rational experimental data which is obtained with care and accuracy.



a) Edge b) Face c) Wall d) Cross section of meshed Cylinder (in y-x plane, at z=0) e) A slice of meshed cylinder (in x-z plane) at mid-y axis, showing 3D elements f) Fully meshed volume

**Fig. 1: Meshing of Chamber**

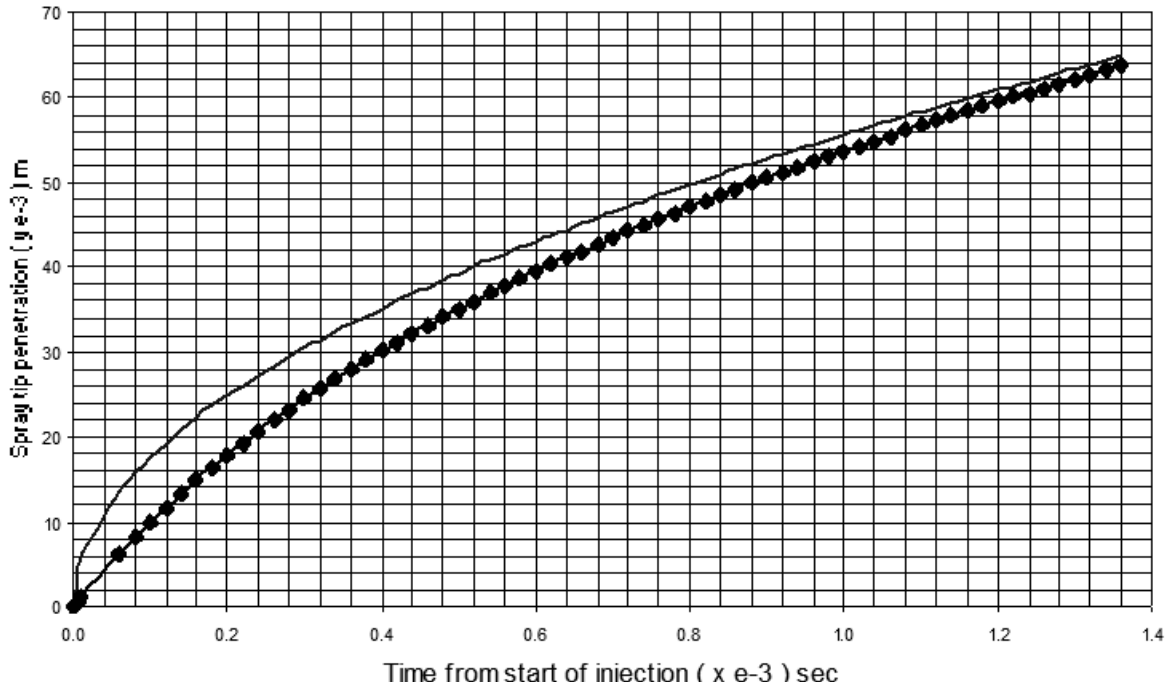


**Fig. 2: Comparison of prediction and experiment**

( $P_{inj}=22$  MPa,  $P_{air}= 2.25$  MPa,  $Dia=0.25$  mm, air density= $27$  kg/cub. m,  
 Chamber air temperature =  $290$  K, fuel density= $850$  kg/m<sup>3</sup>  
 Upper curve is correlation prediction, lower is experimental data)

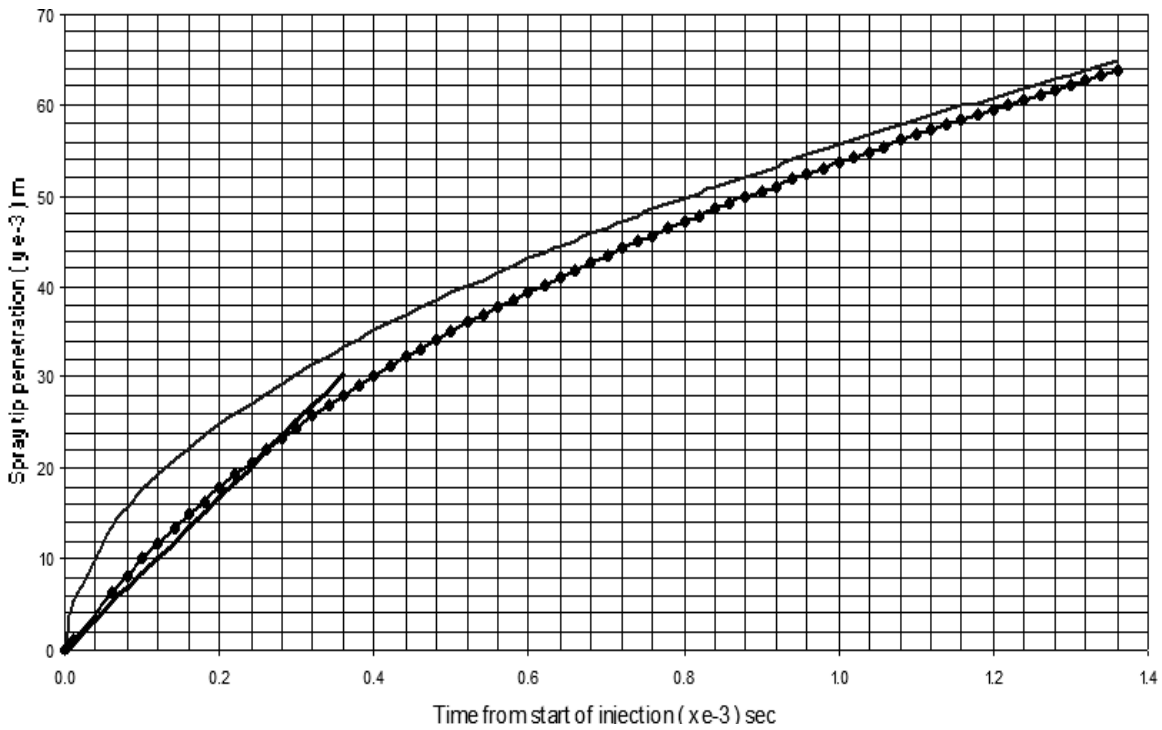


**Fig. 3: Modeling of near nozzle tip zone of spray**

(Upper curve is correlation prediction, Lower curve is experimental data and straight line represents initial liquid zone modeling)

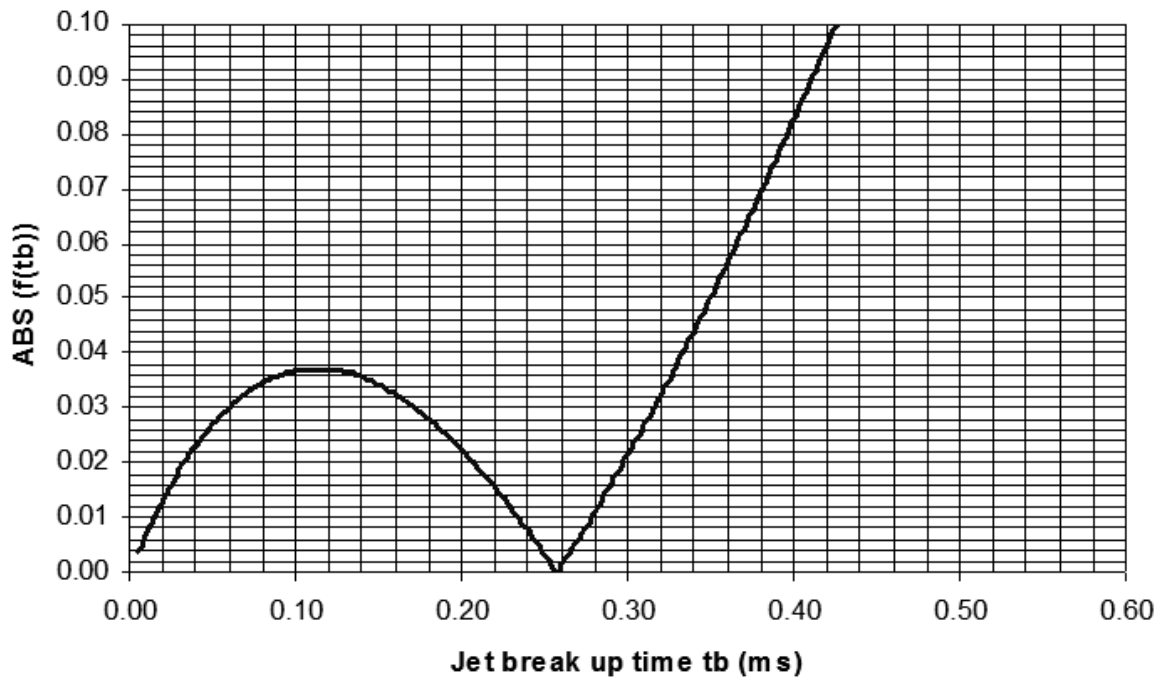


**Fig. 4: Iterative solution for Jet break up time**

( $P_{inj}=22$  MPa,  $P_{air}= 2.25$  MPa, Dia=0.25 mm, air density=27 kg/ m<sup>3</sup>,  
Temp= 290 K, fuel density= 850 kg/ m<sup>3</sup>)

Note: Figures 2-4 are re-produced by the special permission from [7]

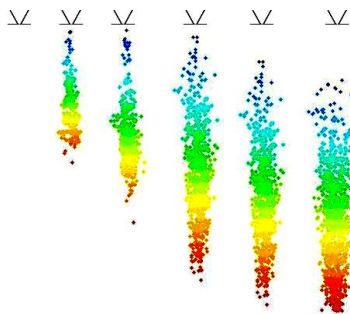


**Fig. 5: Spray shape, at 0.3ms interval, colored by penetration**

( $P_{ch}$  2.25MPa,  $P_{inj}$  22MPa, Nozzle dia 0.25mm, Temperature 290k)

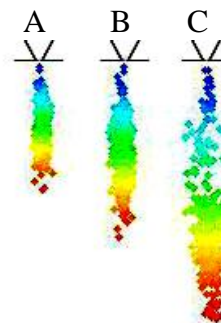


**Fig. 6: Spray Shape**

A = 3.3 B = 2.25 C = 1.2 MPa Chamber pressure, All at time  $t = 0.5$  ms from start of injection

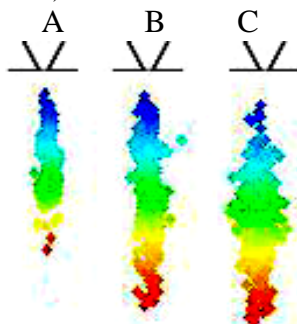


**Fig. 7: Spray Shape**

A = 25 B = 30 C = 40 MPa Injection pressure, All at time  $t = 0.5$  ms from start of injection

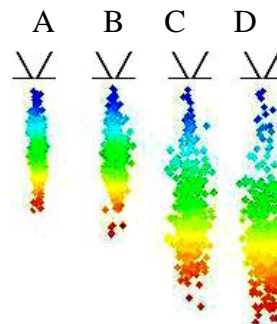
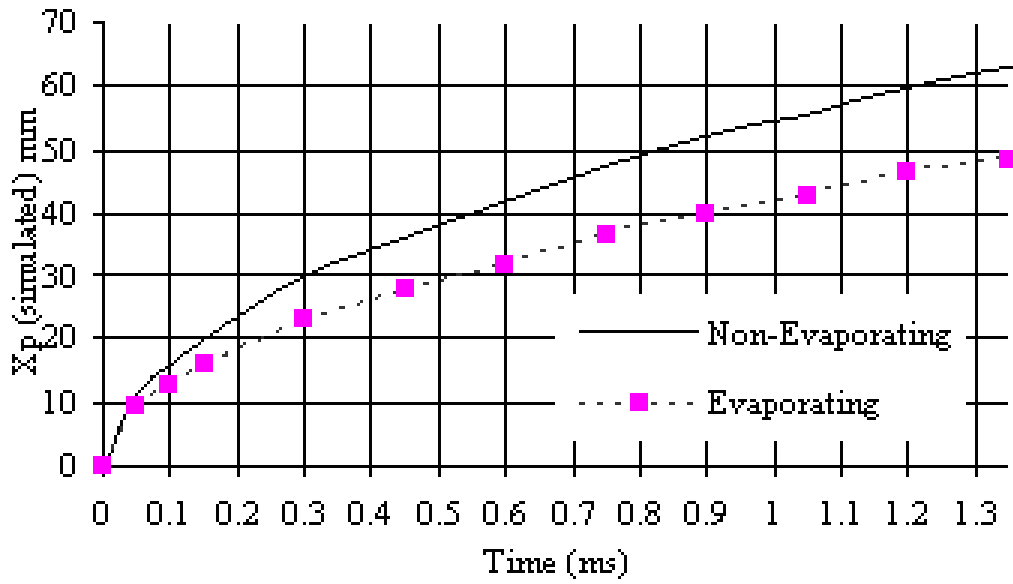


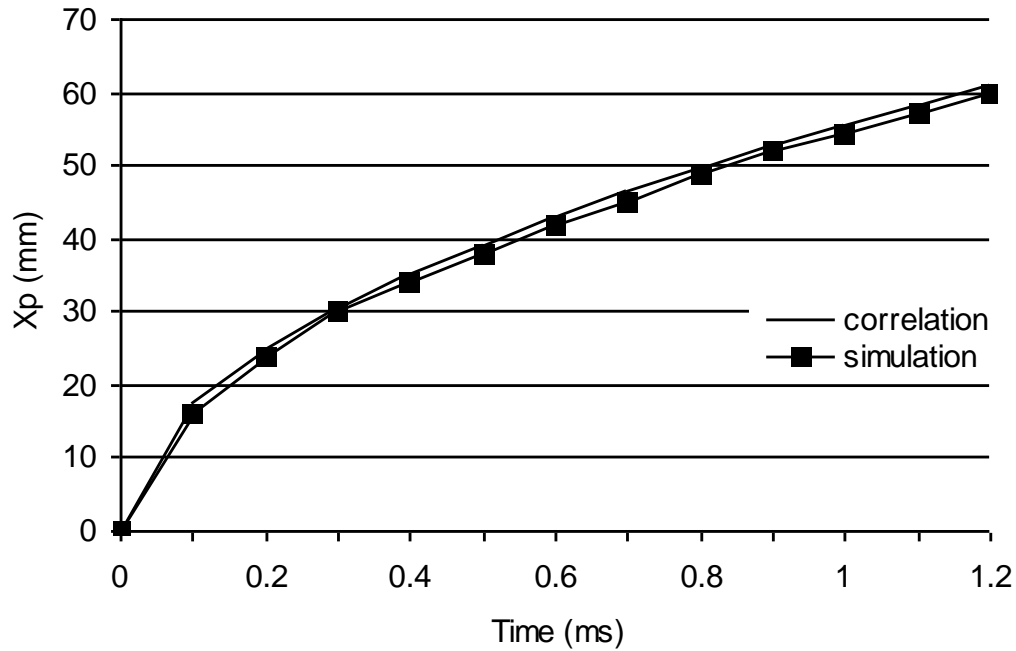
**Fig. 8: Spray Shape**

A = 0.15 B = 0.3 C = 0.4 D = 0.5 mm nozzle diameter All at time  $t = 0.5$  ms from start of injection



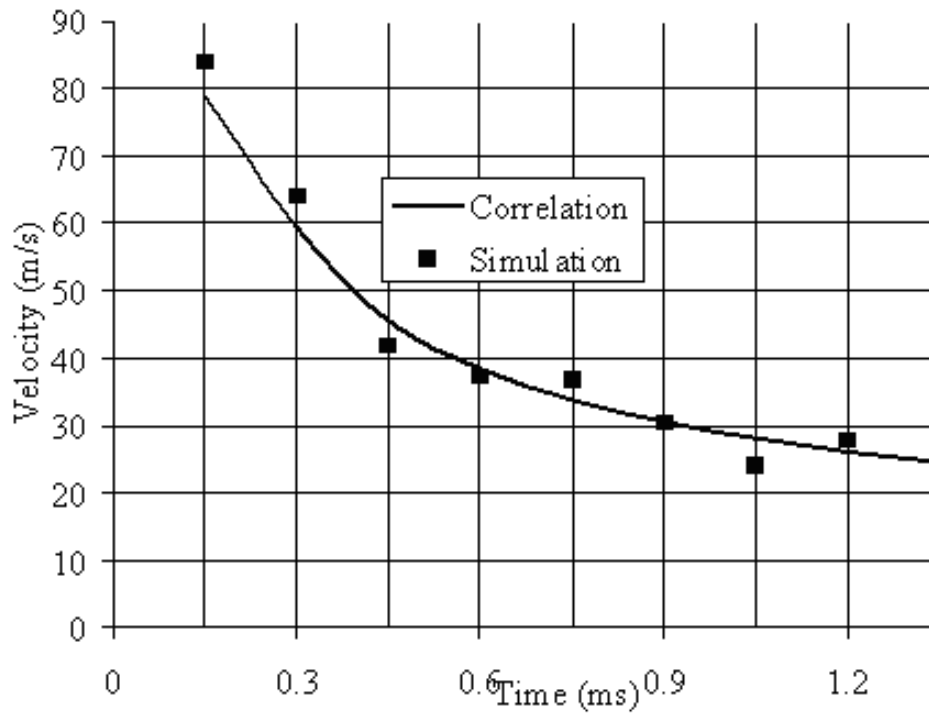
Temp 290K for non-evaporating and 800K for evaporating spray

**Fig. 9: Spray Tip Penetration vs Time**



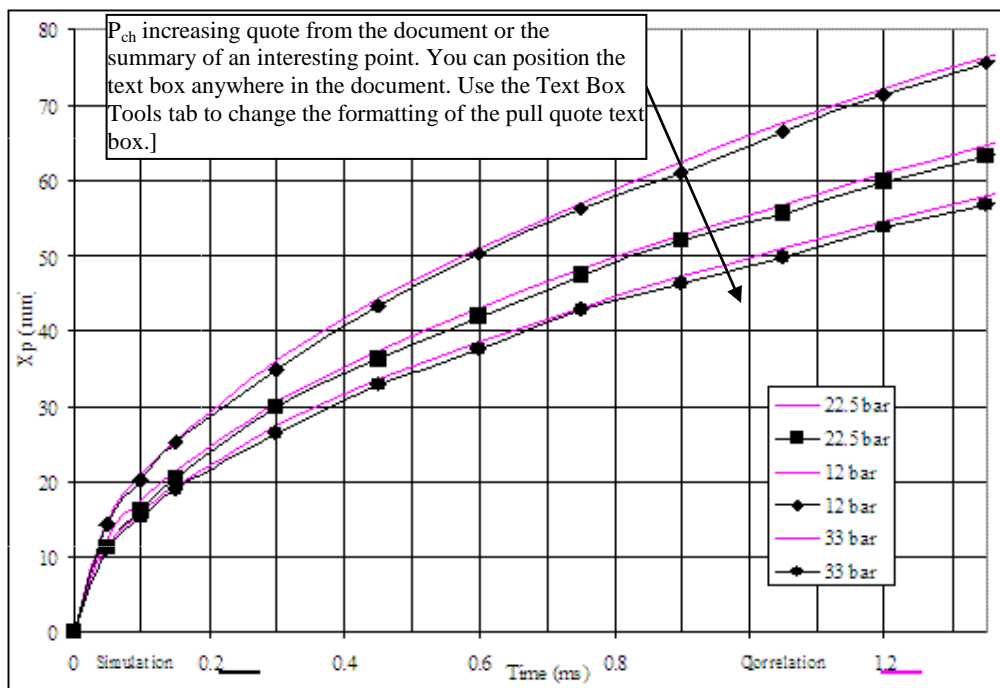
Pch 2.25MPa, Pinj 22MPa, Nozzle dia 0.25mm, Temp 290k

**Fig. 10: Spray Tip Penetration vs Time**



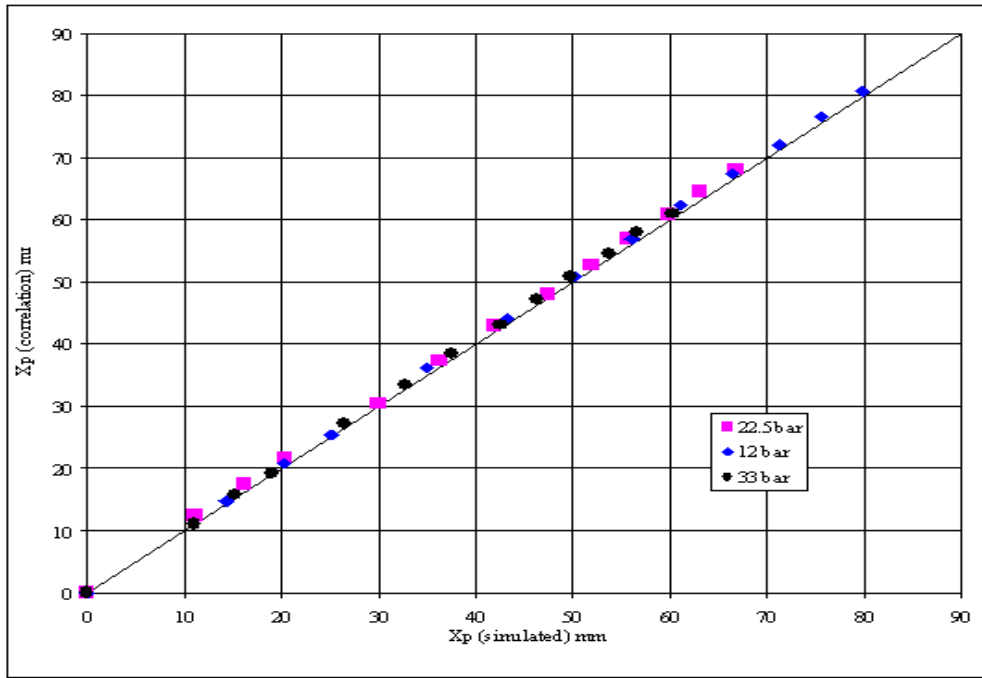
$P_{ch}$  2.25MPa,  $P_{inj}$  22MPa, Nozzle dia 0.25mm, Temp 290k

**Fig. 11: Penetration Velocity ( $V_p$ ) vs Time**



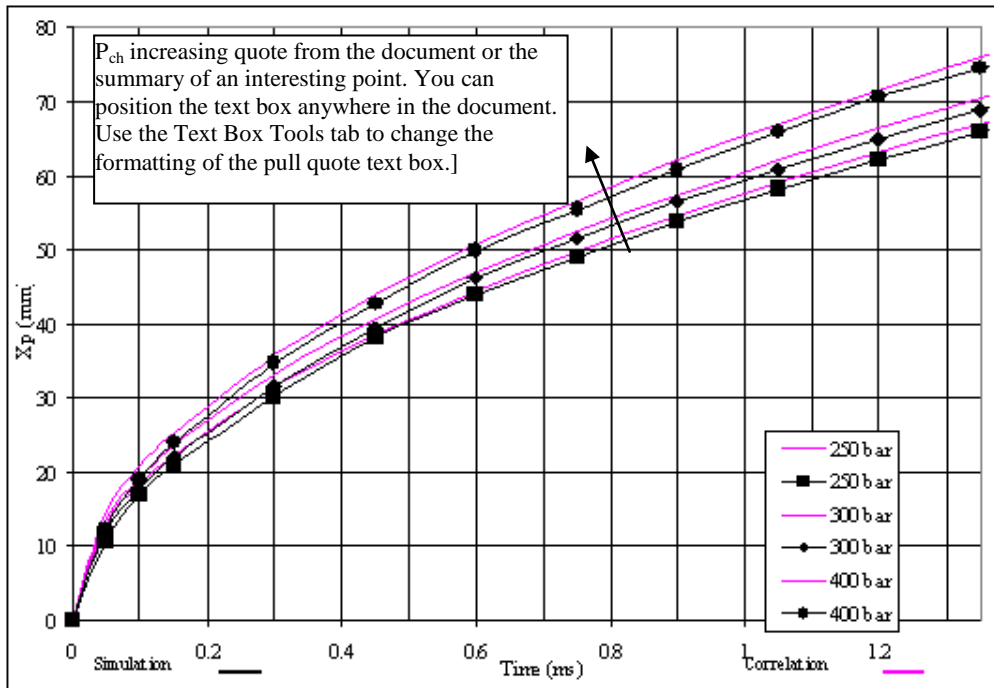
$P_{ch}$  varied,  $P_{inj}$  22MPa, Nozzle dia 0.25mm, Temperature 290k

**Fig. 12: Penetration  $X_p$  (mm) Vs Time (ms)**



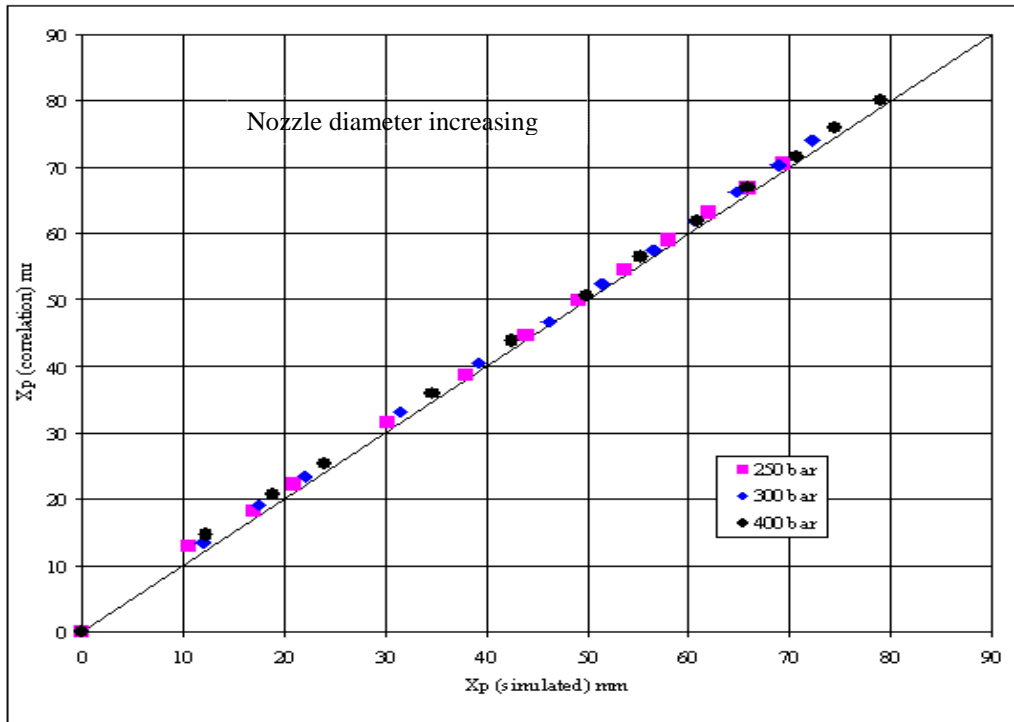
P inj 22MPa, Nozzle diameter 0.25mm, Temperature 290k

Fig. 13: Penetration (correlation) Vs Penetration (simulation)



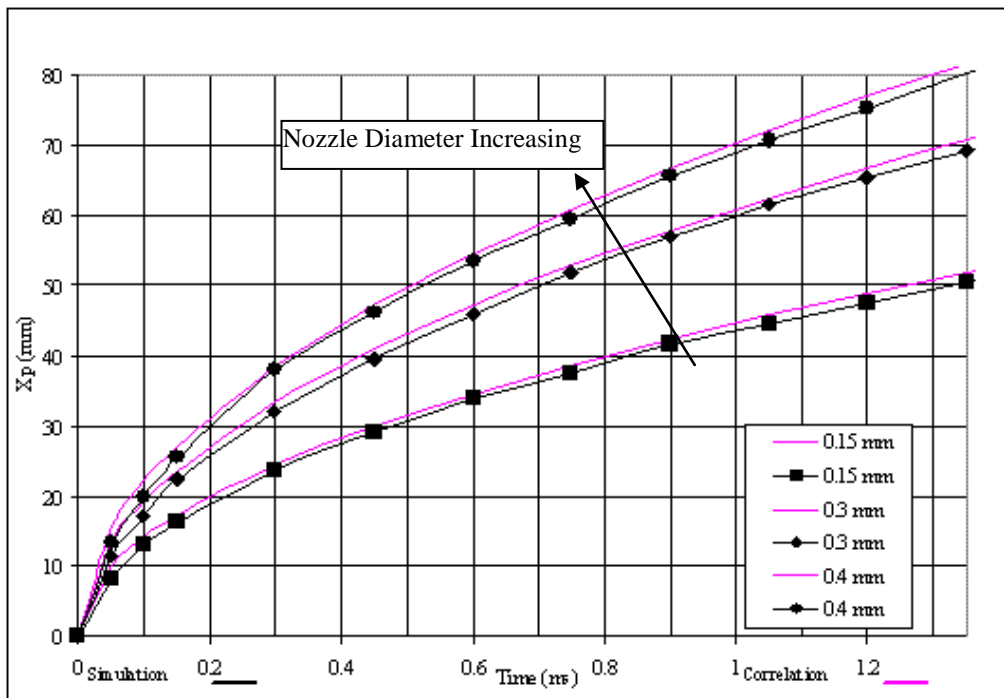
P inj varied, P ch 2.25MPa, Nozzle diameter 0.25mm, Temperature 290k

Fig. 14: Penetration Xp (mm) Vs Time (ms)



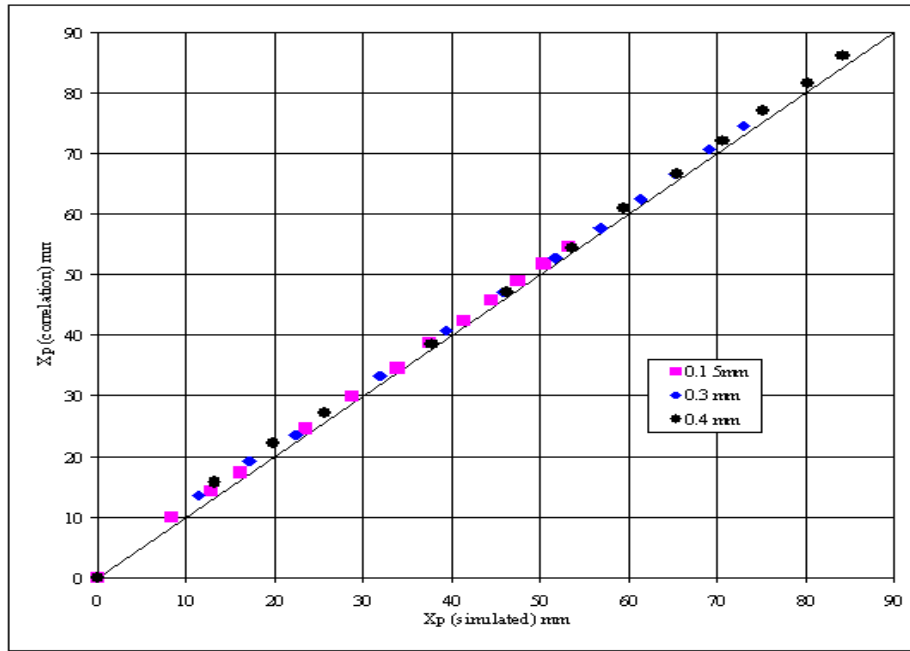
P ch 2.25MPa, Nozzle diameter 0.25mm, Temperature 290k

**Fig. 15: Penetration (correlation) Vs Penetration (simulation)**



P ch 2.25MPa, P inj 22MPa, Nozzle dia varied, mm, Temp. 290k

**Fig. 16: Penetration (correlation) Vs Penetration (simulation)**



P ch 2.25MPa, P inj 22MPa, Nozzle dia 0.25mm, Temp. 290k

**Fig. 17: Penetration (Correlation) Vs Penetration (simulation)**

**Table 1: Fuel and Air properties**

Fuel		Air	
Fuel density	850 kg/m <sup>3</sup>	Air density	27.03 kg/m <sup>3</sup>
Fuel viscosity	0.00332 kg/m.s	Air viscosity	1.789 x10 <sup>-05</sup> kg/m.s
Fuel surface tension	0.0190355 N/m		

**References**

[1] Mirza, M. R., “Studies of Diesel sprays interacting with cross flows and solid boundaries”, PhD Thesis, UMIST UK 1991

[2] A. Saario et al. “Heavy fuel oil combustion in a cylindrical laboratory furnace: Measurements and modeling” Fuel 84 (2005) 359–369 www.fuelfirst.com available since 30 October 2004

[3] P. J. O'Rourke. “Collective Drop Effects on Vaporizing Liquid Sprays” PhD thesis, Princeton University, Princeton, New Jersey, 1981

[4] R. D. Reitz. “Mechanisms of Atomization Processes in High-Pressure Vaporizing Sprays”. Atomization and Spray Technology, 3:309-337, 1987.

[5] Hiroyasu, H., and Arai, M., “Structure of fuel spray in Diesel engines”, SAE vol 99, 1990

[6] J. B. Heywood, *Internal combustion engine fundamentals*, McGraw-Hill Book Co., 1988.

[7] M. R. Mirza, A. H. Baluch, Z.R. Tahir; “Structure of non-evaporating diesel sprays” Pak. J. Engg. & Appl. Sci, 2(2008) 1-8

[8] J. C. Dent; SAE, (1971) 71057